

## To the center of cold spot with *Planck*

V. G. Gurzadyan<sup>1,2</sup>, A. L. Kashin,<sup>2</sup>, H. Khachatryan<sup>2</sup>, E. Poghosian<sup>2</sup>, S. Sargsyan<sup>2</sup>, and G. Yegorian<sup>2</sup>

<sup>1</sup> SIA, Sapienza University of Rome, 00185 Rome, Italy  
 e-mail: gurzadyan@yerphi.am

<sup>2</sup> Center for Cosmology and Astrophysics, Alikhanian National Laboratory and Yerevan State University, Yerevan, Armenia

Received 4 February 2014 / Accepted 22 April 2014

### ABSTRACT

The structure of the cold spot, of a non-Gaussian anomaly in the cosmic microwave background (CMB) sky detected earlier by Vielva et al. (2004, ApJ, 609, 22), is studied using the data by *Planck* satellite. The map obtained of the degree of stochasticity (K-map) of CMB for the cold spot, reveals, most clearly in 100 GHz band, a shell-type structure with a center coinciding with the minima of the temperature distribution. The shell structure is non-Gaussian at a  $4\sigma$  confidence level. Such behavior of the K-map supports the void nature of the cold spot. The method applied can be used for tracing voids that have no signatures in redshift surveys.

**Key words.** cosmic background radiation

### 1. Introduction

The cold spot is a non-Gaussianity in the cosmic microwave background (CMB) sky, which since its first detection (Vielva et al. 2004) in *Wilkinson Microwave Anisotropy Probe* (WMAP) data has attracted much attention in the studies with various statistical descriptors of non-Gaussian features in general, as well as in its interpretation (Cruz et al. 2005; Pietrobon et al. 2008; Gurzadyan et al. 2008; Das & Spergel 2009; Vielva 2010; Valkenburg 2012; Rossmanith 2013; Fernandez-Cobos et al. 2013; Copi et al. 2013; Kovetz & Kamionkowski 2013; Zhao 2013; Planck Collaboration XXIII 2014, and references therein).

A void (i.e., an underdense region in the matter distribution) has been discussed as one of the possible interpretations of the properties of the cold spot (Inoue & Silk 2006; Masina & Notari 2009; Inoue 2012; Kovetz & Kamionkowski 2013). The results represented below offer additional support to the void interpretation of the cold spot and are based on the study of the stochasticity (randomness) properties in the temperature data of *Planck* (Planck Collaboration XXIII 2014). Owing to the hyperbolicity of null geodesics the degree of randomness towards the walls of a void has to be higher than in its inner region (Gurzadyan & Kocharyan 2009a). This property of the cold spot has already been noticed in the WMAP data (Gurzadyan et al. 2009), and as several other sky regions with similar properties have been identified. The randomness of the CMB signal has been studied (Gurzadyan & Kocharyan 2008) using the Kolmogorov stochasticity parameter (Kolmogorov 1933; Arnold 2008, 2009a,b), which enables determining the degree of randomness in the given sequence of real numbers. That method enabled us to reveal X-ray galaxy clusters in *XMM-Newton* data (Gurzadyan et al. 2011b) and to detect the thermal trust Yarkovsky-Rubincam effect for the satellites measuring the Lense-Thirring effect predicted by general relativity (Gurzadyan et al. 2013).

Here we show that the Kolmogorov map (K-map) of *Planck*'s 100 GHz data reveal a shell-like structure in the central region of the cold spot, and this supports its void nature.

### 2. Hyperbolicity

We consider the behavior of null geodesics in underdense regions (cf. Zel'dovich 1964). The equation of geodesic deviation for perturbed Friedmann-Robertson-Walker metric can be reduced to (Gurzadyan & Kocharyan 2009a)

$$\frac{d^2\ell}{dl^2} + r \ell = 0, \quad (1)$$

where  $l$  is the deviation scalar,

$$\lambda(z, \Omega_\Lambda, \Omega_m) = \int_0^z \frac{d\xi}{\sqrt{\Omega_\Lambda + [1 - \Omega_\Lambda + \Omega_m \xi] (1 + \xi)^2}}, \quad (2)$$

and  $\Omega_\Lambda$  and  $\Omega_m$  are the density parameters for the dark energy and matter, respectively. For flat FRW metric the scalar  $r$  has the form

$$r = 2\Omega_m \delta_0, \quad (3)$$

where

$$\delta_0 \equiv \frac{\delta\rho_0}{\rho_0}, \quad (4)$$

and  $\delta\rho_0$  is the local density contrast with respect to the mean matter density  $\rho_0$ .

For voids,

$$\delta_{\text{void}} = \frac{\rho_{\text{void}} - \rho_0}{\rho_0}$$

is negative, thus ensuring the hyperbolicity of null geodesics; i.e., the low density contrast locally acts as a negative curvature, even in a flat universe.

### 3. K-maps

The randomness induced by the hyperbolicity of null geodesics can be studied using CMB data and the Kolmogorov stochasticity parameter (Kolmogorov 1933; Arnold 2008, 2009a,b). The latter is defined for  $\{X_1, X_2, \dots, X_n\}$  real-valued variables  $X$  represented as  $X_1 \leq X_2 \leq \dots \leq X_n$ . For such a sequence the empirical distribution function  $F_n(x)$  is given as

$$F_n(x) = \begin{cases} 0, & x < X_1; \\ k/n, & X_k \leq x < X_{k+1}, \quad k = 1, 2, \dots, n-1; \\ 1, & X_n \leq x, \end{cases}$$

and the cumulative distribution function (CDF) is  $F(x) = P\{X \leq x\}$ . The stochasticity parameter  $\lambda_n$  is estimated as  $\lambda_n = \sqrt{n} \sup_x |F_n(x) - F(x)|$ .

According to Kolmogorov's theorem (Kolmogorov 1933), one has the limit  $\lim_{n \rightarrow \infty} P\{\lambda_n \leq \lambda\} = \Phi(\lambda)$ , for continuous CDF, so that  $\Phi(0) = 0$ , and

$$\Phi(\lambda) = \sum_{k=-\infty}^{+\infty} (-1)^k e^{-2k^2\lambda^2}, \quad \lambda > 0, \quad (5)$$

and  $\Phi$  is independent on  $F$ . The interval  $0.3 \leq \lambda_n \leq 2.4$  corresponds to the variation scale of  $\Phi$  as of objective measure of degree of randomness.

This approach has been applied for several sequences of the theory of dynamical systems and number theory (Arnold 2008, 2009a,b; Atto et al. 2013) and for extensive modeling of generated systems (see Gurzadyan et al. 2011c, and references therein). In the applications to CMB in view of its Gaussian feature, the Gaussian CDF was used for analyzing of the temperature sequences. The obtained Kolmogorov CMB maps (K-maps) for WMAP data readily reveal, for example, the Galactic disk and point sources (galaxies, quasars) that have different randomness (correlation) properties than the cosmological signal (Gurzadyan et al. 2009), thus justifying the efficiency and predictive power of the approach.

The randomness of the cold spot has also been studied for WMAP data using this technique, and the results correspond to features expected for voids, i.e. underdense regions, with the increase in randomness toward their walls (Gurzadyan et al. 2009). Also, a sample of regions has been revealed in the CMB sky, with similar behavior, although less outlined, of the function  $\Phi$  vs. the radius.

We now analyze the cold spot region using *Planck*'s temperature data (nominal) in HEALPix format (Gorski et al. 2005). The computations were performed in the following manner (for details see Gurzadyan et al. 2009). The temperature data sequences in ball regions of radius 0.5 degree located at step 0.05 degree have been chosen, containing about 950 pixels each for 100 GHz  $N_{\text{side}} = 2048$  maps, and for them the function  $\Phi$  has been obtained. The stability of the results was tested by varying the input parameters, most importantly the step (varying it e.g. within 0.01–0.05 degree) and the radius (see also Gurzadyan et al. 2009), thus ensuring the robustness of the results.

First, using the temperature cuts for the cold spot region, we determined the minima of the 100 GHz temperature plots, possessing the coordinates  $(210.04^\circ, -56.26^\circ)$ , as shown in Fig. 1. Then, in Fig. 2 we represent the 100 GHz temperature  $N_{\text{side}} = 2048$  map (in  $\mu\text{K}$  scale, upper plot) and the corresponding K-map for the cold spot region, with denoted temperature minima location. A shell-like structure with a 0.6 degree radius of external boundary is visible in the K-map, which is absent

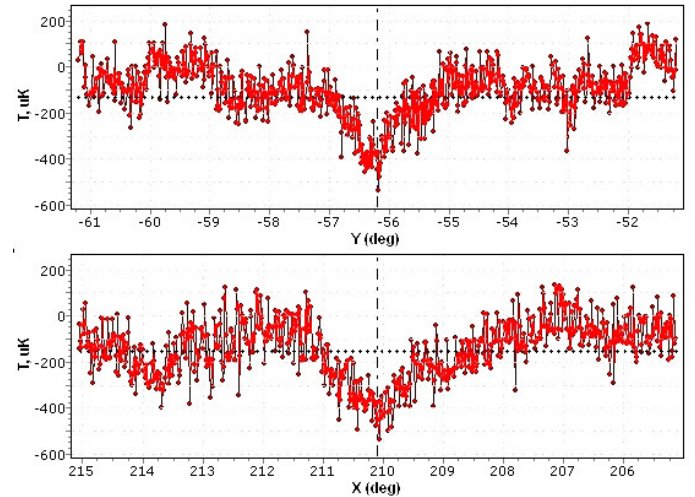


**Fig. 1.** Temperature run vs. latitude and longitude for the cold spot region for *Planck*'s 100 GHz map.

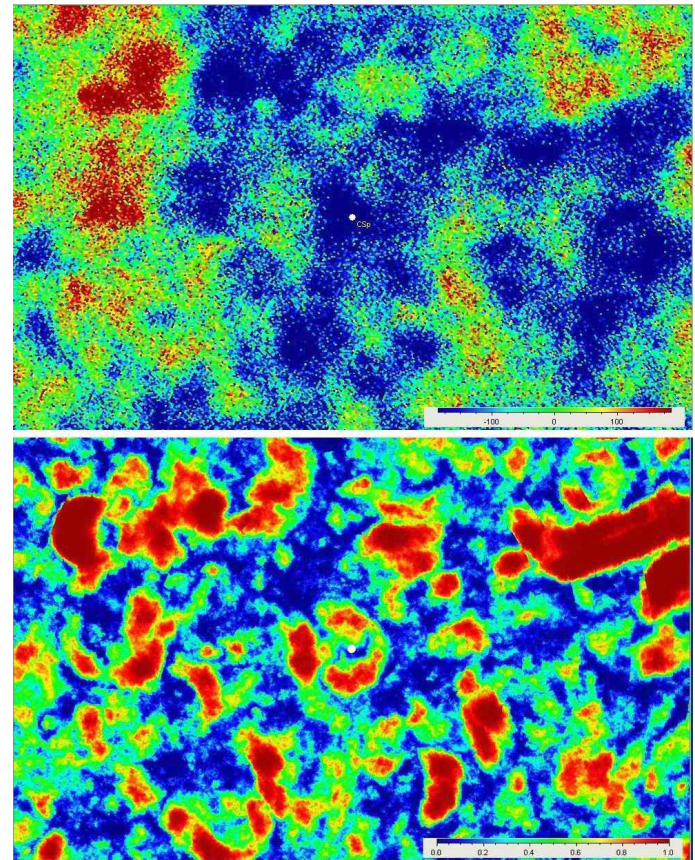


**Fig. 2.** 100 GHz temperature map (above) and its K-map. The denoted point of coordinates  $(210.04^\circ, -56.26^\circ)$  corresponds to the minima of the temperature run in Fig. 1.

in the temperature map and clearly surrounds the “center” defined by temperature minima. The same shell structure is also available in 143 GHz K-map (Fig. 3), again without a trace in its temperature map, but has no such outlined signature in  $N_{\text{side}} = 2048$  70 GHz K-map (Fig. 4). To quantify the confidence level of the shell, we used the same algorithm to estimate the behavior of  $\Phi$  vs. the radius for 200 regions of a Gaussian map with  $T_{\text{mean}} = 27.47 \mu\text{K}$  and  $\sigma = 119.99 \mu\text{K}$  of the *Planck*'s 100 GHz map of the northern sky without the Galactic disk

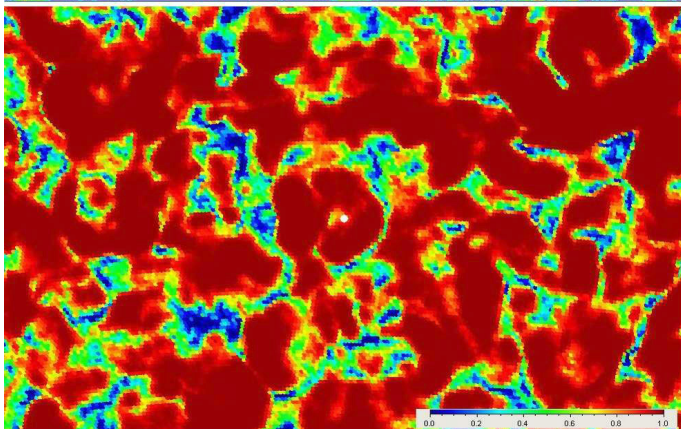
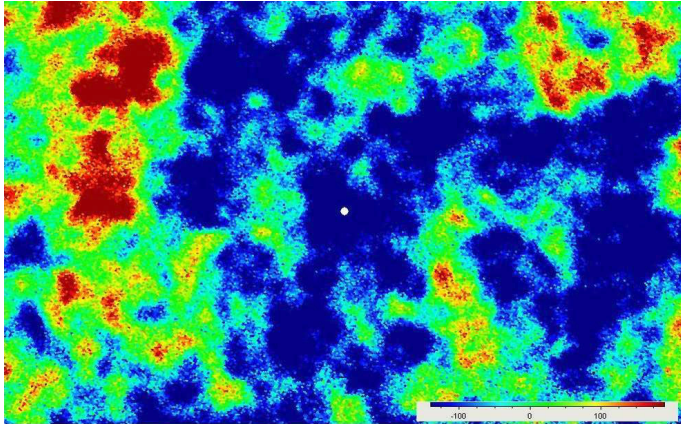


**Fig. 3.** Same as in Fig. 2 but for 143 GHz.

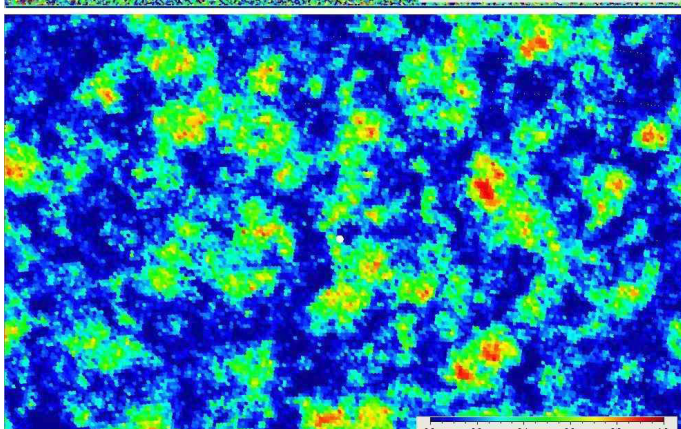
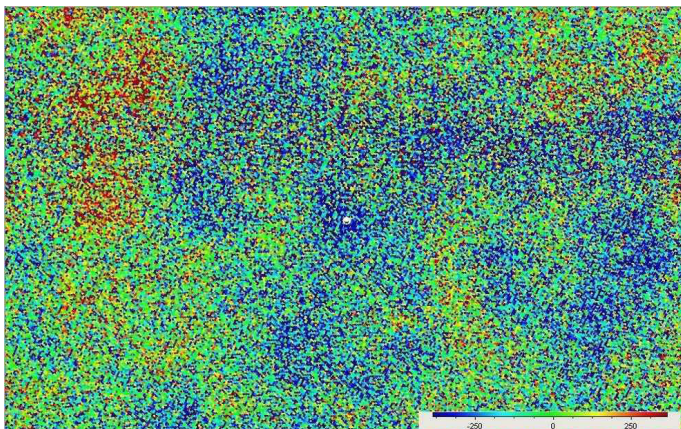


**Fig. 4.** Same as in Fig. 2 but for 70 GHz.

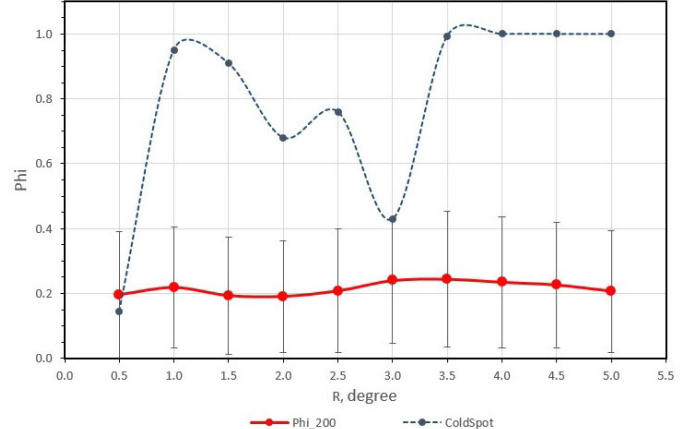


**Fig. 5.** Dependence of  $\Phi$  vs. the radius for the cold spot for 100 GHz data and for 200 regions of simulated Gaussian map of the parameters of the 100 GHz map (more in the text).

region ( $|b| < 20$  degree). As seen from Fig. 5, the jump of  $\Phi$  of the cold spot yields over  $4\sigma$  [ $(0.95-0.14)/0.2$ ].

#### 4. Conclusions

We have studied the structure of the cold spot using the *Planck* CMB temperature maps and obtained the corresponding K-maps, i.e., the distribution of the degree of randomness in that region. The quality of *Planck* data enabled us to reveal in the 100 GHz K-map a shell-like structure, the center of which does coincide with the position of the temperature minima. Such a shell structure is also clear in 143 GHz K-map but has no such visible trace in the 70 GHz K-map ( $N_{side} = 2048$ ).

The shell-type distribution of the degree of randomness is expected at the hyperbolicity of null geodesics induced by voids. The obtained structure in the K-map does therefore support the void nature of the cold spot. It is worth mentioning that the universality of the applied method enables a void to be traced independently of whether its walls are outlined well by luminous matter or mostly contain dark matter, hence have no clear correlations with available galaxy redshift surveys (Bremer et al. 2010; Granett et al. 2010). The void of the cold spot, therefore, may need more refined alternative means for study. The importance of the presence of voids with determined parameters is obvious for understanding the formation of large scale structure in the universe.

*Acknowledgements.* We acknowledge the useful comments by the referee and the use of *Planck* data (<http://pla.esac.esa.int/pla/aio/planckProducts>).

#### References

- Arnold, V. I. 2008, *Uspekhi Mat. Nauk*, 63, 5
- Arnold, V. I. 2009a, *Trans. Moscow Math. Soc.*, 70, 31
- Arnold, V. I. 2009b, *Funct. An. Other Math.*, 2, 139
- Atto, A. M., Berthoumieu, Y., & Megret, R. 2013, *Entropy*, 15, 4782
- Bremer, M. N., Silk, J., Davies, L. J. M., & Lehnert, M. D. 2010, *MNRAS*, 404, L69
- Copi, C. J., Huterer, D., Schwarz, D. J., & Starkman G. D. 2013, *MNRAS*, submitted [[arXiv:1311.4562](https://arxiv.org/abs/1311.4562)]
- Cruz, M., Martinez-Gonzalez, E., Vielva, P., & Cayton, L. 2005, *MNRAS*, 356, 29
- Das, S., & Spergel, D. N. 2009, *Phys. Rev. D*, 79, 3007

- Fernandez-Cobos, R., Vielva, P., Martinez-Gonzalez, E., Tucci, M., & Cruz, M. 2013, MNRAS, 435, 3096
- Gorski, K. M., Hivon, E., Banday, A. J., et al. 2005, ApJ, 622, 759
- Granett, B. R., Szapudi, I., & Neyrinck, M. C. 2010, ApJ, 714, 825
- Gurzadyan, V. G., & Kocharyan, A. A. 2008, A&A, 492, L33
- Gurzadyan, V. G., & Kocharyan A. A. 2009a, A&A, 493, L61
- Gurzadyan, V. G., & Kocharyan A. A. 2009b, Europhys. Lett., 86, 29002
- Gurzadyan, V. G., Starobinsky, A. A., Ghahramanyan, T., et al. 2008, A&A, 490, 929
- Gurzadyan, V. G., Allahverdyan, A. E., Ghahramanyan, T., et al. 2009, A&A, 497, 343
- Gurzadyan, V. G., Allahverdyan, A. E., Ghahramanyan, T., et al. 2011a, A&A, 525, L7
- Gurzadyan, V. G., Durret, F., Ghahramanyan, T., et al. 2011b, Europhys. Lett., 95, 69001
- Gurzadyan, V. G., Ghahramanyan, T., & Sargsyan, S. 2011c, Europhys. Lett., 95, 19001
- Gurzadyan, V. G., Ciufolini, I., Sargsyan, S., et al. 2013, Europhys. Lett., 102, 60002
- Inoue, K. T. 2012, MNRAS, 421, 2731
- Inoue, K. T., & Silk, J. 2006, ApJ, 648, 23
- Kolmogorov, A. N. 1933, G. Ist. Ital. Attuari, 4, 83
- Kovetz, E. D., & Kamionkowski, M. 2013, Phys. Rev. Lett., 110, 171301
- Masina, I., & Notari, A. 2009, JCAP, 7, 35
- Pietroni, D., Amblard, A., Balbi, A., et al. 2008, Phys. Rev. D, 78, 103504
- Planck Collaboration, XXIII 2014, A&A, in press,

[DOI: 10.1051/0004-6361/201321534](https://doi.org/10.1051/0004-6361/201321534)

Rosmanith, G. 2013, Non-linear Data Analysis on the Sphere (Springer)

Valkenburg, W. 2012, JCAP, 01, 047

Vielva, P. 2010, Adv. Astr., id. 592094

Vielva, P., Martinez-Gonzalez, E., Barreiro, R. B., et al. 2004, ApJ, 609, 22

Zel'dovich, Ya. B. 1964, Astron. Zh. 41, 19

Zhao, W. 2013, MNRAS, 433, 3498